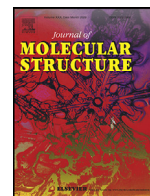




Since January 2020 Elsevier has created a COVID-19 resource centre with free information in English and Mandarin on the novel coronavirus COVID-19. The COVID-19 resource centre is hosted on Elsevier Connect, the company's public news and information website.

Elsevier hereby grants permission to make all its COVID-19-related research that is available on the COVID-19 resource centre - including this research content - immediately available in PubMed Central and other publicly funded repositories, such as the WHO COVID database with rights for unrestricted research re-use and analyses in any form or by any means with acknowledgement of the original source. These permissions are granted for free by Elsevier for as long as the COVID-19 resource centre remains active.



Synthesis, spectroscopic and computational characterization of charge transfer complex of remdesivir with chloranilic acid: Application to development of novel 96-microwell spectrophotometric assay

Ibrahim A. Darwish^{a,*}, Nasr Y. Khalil^a, Hany W. Darwish^{a,b,*}, Nourah Z. Alzoman^a, Abdullah M. Al-Hossaini^a

^a Department of Pharmaceutical Chemistry, College of Pharmacy, King Saud University, P.O. Box 2457, Riyadh 11451, Saudi Arabia

^b Department of Analytical Chemistry, Faculty of Pharmacy, Cairo University, Kasr El-Aini St., Cairo 11562, Egypt

ARTICLE INFO

Article history:

Received 4 March 2022

Revised 12 April 2022

Accepted 13 April 2022

Available online 17 April 2022

Keywords:

Remdesivir

Chloranilic acid

Charge transfer complex

Spectroscopy

96-microwell assay

ABSTRACT

Remdesivir (REM) is an adenosine triphosphate analog antiviral drug that has received authorization from European Commission and approval from the U.S. Food and Drug Administration for treatment of coronavirus disease 2019 (Covid-19). This study, describes, for the first time, the synthesis of a novel charge transfer complex (CTC) between REM, as electron donor, with chloranilic acid (CLA), as π electron acceptor. The CTC was characterized using different spectroscopic and thermogravimetric techniques. UV-visible spectroscopy ascertained the formation of the CTC in methanol via formation of a new broad absorption band with maximum absorption peak (λ_{max}) at 530 nm. The molar absorptivity (ϵ) of the complex was 3.33×10^3 L mol⁻¹ cm⁻¹ and its band gap energy was 1.91 eV. The stoichiometric ratio of REM:CLA was found to be 1:1. The association constant of the complex was 1.11×10^9 L mol⁻¹, and its standard free energy was 5.16×10^4 J mole⁻¹. Computational calculation for atomic charges of energy minimized REM was conducted, the site of interaction on REM molecule was assigned and the mechanism of the reaction was postulated. The solid-state CTC was further characterized by FT-IR and ¹H NMR spectroscopic techniques. Both FT-IR and ¹H NMR confirmed the formation of the CTC and its structure. The reaction was adopted as a basis for developing a novel 96-microwell spectrophotometric method (MW-SPA) for REM. The assay limits of detection and quantitation were 3.57 and 10.83 μ g/well, respectively. The assay was validated, and all validation parameters were acceptable. The assay was implemented successfully with great precision and accuracy to the determination of REM in its bulk form and pharmaceutical formulation (injection). This assay is simple, economic, and more importantly, has high throughput property. Therefore, the assay can be valuable for routine in quality control laboratories for analysis of REM's bulk form and pharmaceutical injection.

© 2022 Elsevier B.V. All rights reserved.

1. Introduction

Mulliken [1] was the first to coin the term charge transfer complex (CTC), which was later widely discussed by Foster [2]. The electronic charge is partially transferred from an electron donor molecule to an electron acceptor molecule during the production of CTC [1–3]. CTC formation chemistry is crucial in a wide range of chemical and biochemical sciences, bio-electrochemical energy transfer procedures, biological systems and pharmaceutical manufacturing processes. Possible drug-receptor binding interactions,

enzyme catalysis, and substance transport through lipophilic membranes in bodily compartments, for example, have all been thoroughly characterized by investigating charge transfer complex interactions [4–9]. CTC creation is also crucial in a multitude of fields, including the production of optical and electrically conductive materials [10–13], microemulsions and surface chemistry [14], photocatalysis [15], dendrimers [16], solar energy storage [17], and organic semiconductors [18]. Additionally, the generation of CTC between drugs and specific σ - and π -acceptors has been effectively employed as the basis for designing high-accuracy assays for both qualitative and quantitative detection of pharmaceuticals in bulk and/or pharmaceutical dose forms [19–30].

We've been evaluating the development and applications of CTC in a variety of pharmaceuticals with diverse acceptors over the past few years. Antibiotics, kinase inhibitors, antihypertensives

* Correspondence authors at: Department of Pharmaceutical Chemistry, College of Pharmacy, King Saud University, P.O. Box 2457, Riyadh 11451, Saudi Arabia.

E-mail addresses: idarwish@ksu.edu.sa (I.A. Darwish), hdarwish@ksu.edu.sa (H.W. Darwish).

and antihyperlipidemics were among the pharmaceuticals used [19–30]. Our research focused on understanding the chemistry of these pharmaceuticals' CT reactions and their electron donating manners toward a variety of electron acceptors. The features of CT complexes have been thoroughly examined, as have the conditions under which they arise.

In the present work, we examined the CT reaction of CLA with remdesivir (REM). REM is an adenosine triphosphate analogue with broad-spectrum antiviral activity medication. It has been developed by the biopharmaceutical company Gilead Sciences Inc. (Foster City, California, United States) and sold under the brand name Veklury® injection (100 mg/vial). REM has been first described in 2016 as a potential treatment for Ebola. It has demonstrated in vitro and in vivo activity against the viral pathogens MERS and SARS, which are also coronaviruses and are structurally similar to Covid-19 [31]. On May 1, 2020, REM has received conditional marketing authorization from the European Medicines Agency (EMA) for the treatment of the entire population with coronavirus disease 2019 (Covid-19) [32]. On October 22, 2020, the U.S. Food and Drug Administration (FDA) approved REM for use in adult and pediatric patients 12 years of age and older and weighing at least 40 kgs (about 88 pounds) for the treatment of COVID-19 requiring hospitalization [33].

The therapeutic effectiveness of REM, as well as the existence of numerous potentially electron-donating sites on its structure (nitrogen and carbonyl oxygen atoms), sparked our curiosity in understanding more about the chemistry of REM's CT interaction. These locations allow REM to form CTC with electron acceptors. Chloranilic acid (CLA) was shown to be the most reactive electron acceptor in our earlier investigations employing a variety of polyhalo/polycyanoquinone electron acceptors [34,35]. CLA reaction, in most cases, is immediate at ambient temperature.

In the current work, first, REM was reacted with CLA in various organic solvents, the reaction conditions were adjusted, the complex's association constant as well as the reaction's molar ratio were calculated. The solid-state complex was then synthesized, and its molecular composition was determined using UV-visible, mass, FT-IR, and ^1H NMR spectroscopy. Afterwards, based on computational calculations and spectroscopic data, the reaction mechanism was proposed. Lastly, the CT reaction has been used to establish a new 96-microwell assay with high throughput for detecting REM in bulk and its correspondent dosage form (injection).

2. Experimental

2.1. Apparatus

UV-VIS spectrophotometer (UV-1601 PC: Shimadzu, Kyoto, Japan), double beam with matched 1-cm quartz cells. PerkinElmer FT-IR spectrum BX apparatus (PerkinElmer, Norwalk, CT, USA). Bruker NMR spectrometer (Bruker Corporation, Bruker Daltonik GmbH, Bremen, Germany) operating at 700 MHz. PerkinElmer thermal analyzer (TGA-8000: PerkinElmer, Norwalk, CT, USA). Microplate absorbance reader (ELx808: Bio-Tek Instruments Inc., Winooski, VT, USA) empowered by KC Junior software, provided with the instrument. Transparent non-binding 96-microwell assay plates were a product of Corning/Costar Inc. (Cambridge, MA, USA). An adjustable 8-channel pipette was obtained from Sigma Chemical Co. (St. Louis, MO, USA).

2.2. Chemicals and materials

Remdesivir (REM) was purchased from Weihua Pharma Co., Ltd. (Hangzhou, Zhejiang, China). Veklury® injection (Gilead Sciences, Inc., USA) labelled to contain 100 mg of REM per vial were purchased from the local market. CLA was purchased from Sigma-

Aldrich Corporation (St. Louis, MO, USA). Finnpiptette adjustable single and 8-channel pipettes were procured from Sigma-Aldrich Co. (St. Louis, MO, USA). The solvents and other reagents employed in the study were of analytical grade (Fisher Scientific, California, CA, USA).

2.3. Preparation of REM standard and injection solutions

Stock standard REM solution (5 mg mL^{-1}) was prepared by dissolving an accurately weighed amount (50 mg) of the standard material in 10 mL of methanol. This solution was subsequently diluted with methanol to obtain REM concentrations suitable for each of the particular subsequent experiments. The veklury® injection sample solution was prepared as the following procedure. A quantity of the lyophilized powder of the vial equivalent to 20 mg of REM was transferred into a 10-mL calibrated flask, dissolved in 5 mL methanol, swirled and sonicated for 5 min, completed to volume with methanol, shaken well for 10 min, and filtered. The first part of the filtrate was discarded, and an accurate volume of the filtrate was diluted with methanol to claimed concentrations of 25 and 50 $\mu\text{g/mL}$, the solutions were subjected to the analysis by the proposed MW-SPA.

2.4. Determination of association constant and molar ratio

With a series of CLA solutions (1×10^{-4} – 3.3×10^{-3} M) and a fixed concentration of REM (1.3×10^{-3} M), the Benesi-Hildebrand method [36] was used to calculate the association constant of the CTC. Job's continuous variation method [37] was adopted to calculate the molar ratio of REM:CLA in the reaction. Equimolar solutions (4×10^{-3} M) of REM and CLA reagent were used.

2.5. Synthesis of the solid CTC

Synthesis of the proposed CTC of REM with CLA took place by mixing 10-mL of solutions containing 60.26 mg (0.1 mmol) of REM and 20.9 mg (0.1 mmol) of CLA in methanol. The resulting mixture was allowed to proceed at room temperature (25 ± 2 °C) for 30 min with continual magnetic stirring. The reaction solution was then bubbled with helium gas to vaporize the solvent, and the resulting residue was left to dry over anhydrous calcium chloride in a vacuum desiccator. FT-IR and ^1H NMR spectroscopy were employed to analyze the dried residue.

2.6. MW-SPA procedures

Into each well of the transparent 96-microwell assay plates, 100 microliters of the standard or injection sample solution that contains varied amounts of REM (3.77 – 241 $\mu\text{g/well}$) were transferred. A hundred microliters of CLA solution (0.5%, w/v) have been added, and the reaction was allowed to take place for 5 min at room temperature (25 ± 2 °C). The microwell-plate reader was used to read the absorbances of the solutions at 490 nm.

3. Results and discussion

3.1. UV-Visible absorption spectra and band gap energy

The UV-visible absorption spectra of REM (2×10^{-4} M) and CLA (12×10^{-4} M) solutions were measured between 200 and 800 nm. The spectra of REM clearly show that it has discrete absorption maxima (λ_{max}) at 245 and no UV absorption after 340 nm (Fig. 1). CLA possesses high UV-absorption before 340 nm and weak absorption at 360 – 640 nm (Fig. 1).

Different concentrations of REM solutions (2×10^{-4} – 12×10^{-4} M) were mixed separately with a fixed concentration of

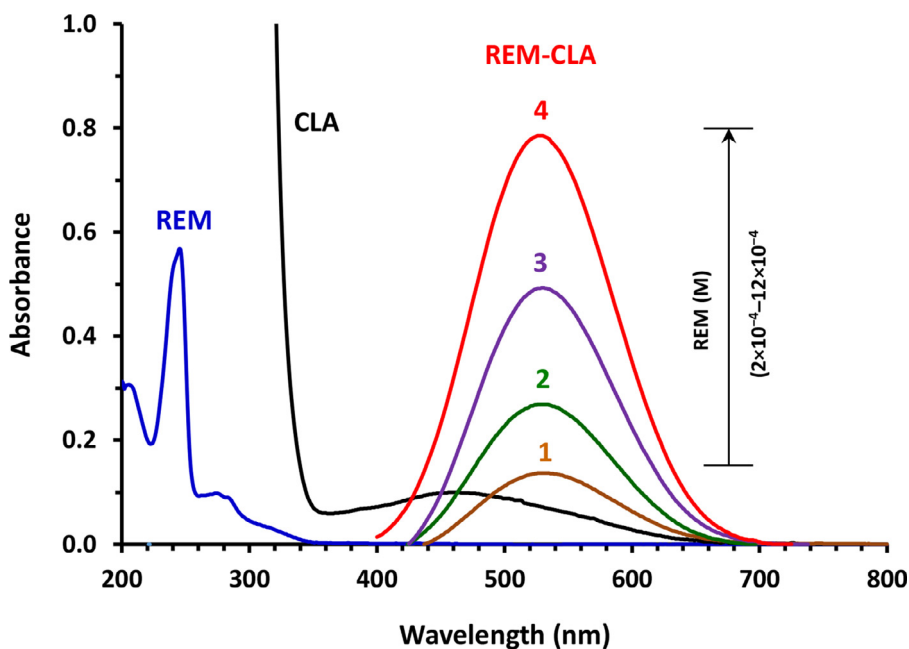
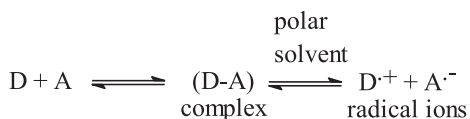


Fig. 1. Absorption spectra of REM (1.66×10^{-5} M), CLA (4.8×10^{-5} M) and reaction mixtures containing varying concentrations of REM (2×10^{-4} M – 12×10^{-4} M) and a fixed concentration of CLA (4×10^{-3} M); all solutions were in methanol. Numbers on the spectra of the reaction mixtures are denoted to the concentrations of REM used in the reaction mixtures. These concentrations were 2×10^{-4} M (1), 4×10^{-4} M (2), 8×10^{-4} M (3) and 12×10^{-4} M (4).

CLA solution (4×10^{-3} M), where their interaction was allowed to go on at 25 ± 2 °C. The absorption spectra of the reaction mixtures were measured versus CLA reagent blank solution (Fig. 1), where an observed violet-colored product was acquired with maximum absorption at 530 nm, and its intensity enlarged with increasing REM concentration (Fig. 1).

This behavior supports the expectation of forming a new reaction product. The absorption band that resulted was identical in pattern and shape to that of the radical anion of CLA reported in the literature [26,34,35]. As a result, the reaction was hypothesized to be a CT interaction between REM as an electron donor (D) and CLA as a π -electron acceptor (A). This reaction was proceeded in a polar solvent such as acetonitrile to form CTC (D-A), which was then dissociated by the forceful ionizing power of acetonitrile to form the radical anion of CLA:



A well-established fact about CLA is that it exists in two stable forms: a purple-colored stable form (HA^-) at pH = 3 [38], and a pale violet form (A^{2-}) that is stable at higher pH [38]. As a result, the purple reaction product formed by the interaction of REM with CLA in acetonitrile was determined to be the HA^- form of CLA that was engaged in the reaction.

It was further established that the reaction was CT by the vanishing of the purple color of the reaction mixture after it was acidified with mineral acids.

The band gap energy (E_g), defined as “the least energy required for the excitation of an electron from the lower energy valence band into the higher energy for participation in forming a conduction band” [39], was computed. An absorption spectrum of the CTC complex was used to construct a Tauc plot (Fig. 2), which was then used to perform E_g calculations. The Tauc plot was created by plotting energy values ($h\nu$, in eV) versus $(\alpha h\nu)^2$. By projecting the linear section of the graph to $(\alpha h\nu)^2 = 0$, we were able to calculate

the value of E_g [40]. According to the results, the calculated value of E_g was found to be 1.91 eV. This small estimated value demonstrates the ease with which electrons flow from REM to CLA and the creation of the CTC absorption band.

3.2. Optimization of the reaction conditions

The reaction of REM with CLA was carried out in various solvents with different dielectric constants [41] and polarity indexes [42] in order to determine the most appropriate solvent for the optimal reaction and color development. For this purpose, the absorption spectra of the resulting color were measured and recorded (Fig. 3). From the acquired spectra, the molar absorptivity (ϵ) and λ_{\max} were recorded in each studied solvent. Slight shifts in the λ_{\max} values and changes in the ϵ values were observed. The reaction in solvents with high polarity and high dielectric constants (such as methanol and acetonitrile) produced higher results than in solvents possesses low polarity and low dielectric constants (e.g. diethyl ether and dichloroethane). This effect may be due to the complete electron transfer from REM molecule (electron donor) to CLA (electron acceptor) that is favoured in the polar solvents. Methanol was the selected solvent in all the subsequent procedures. In methanol, it was found that the reaction proceeded instantaneously at ambient temperature (25 ± 2 °C), as concluded from studying the effect of time on the reaction (Fig. 4).

3.3. Association constant, free energy change and ionization potential

The Benesi-Hildebrand approach [35] was used to calculate the association constant (K_c) at room temperature (25 ± 2 °C) and at the λ_{\max} of the formed REM-CLA complex using the absorption spectra of the complex formed by reacting numerous concentrations of CLA with a fixed concentration of REM (Fig. 5A). Straight line was attained from which the CTC's association constant was calculated (Fig. 5B). The value of the association constant was revealed to be 1.11×10^9 L mol $^{-1}$.

The CTC's standard free energy change (ΔG^0) is proportional to its formation constant and may be calculated using the formula:

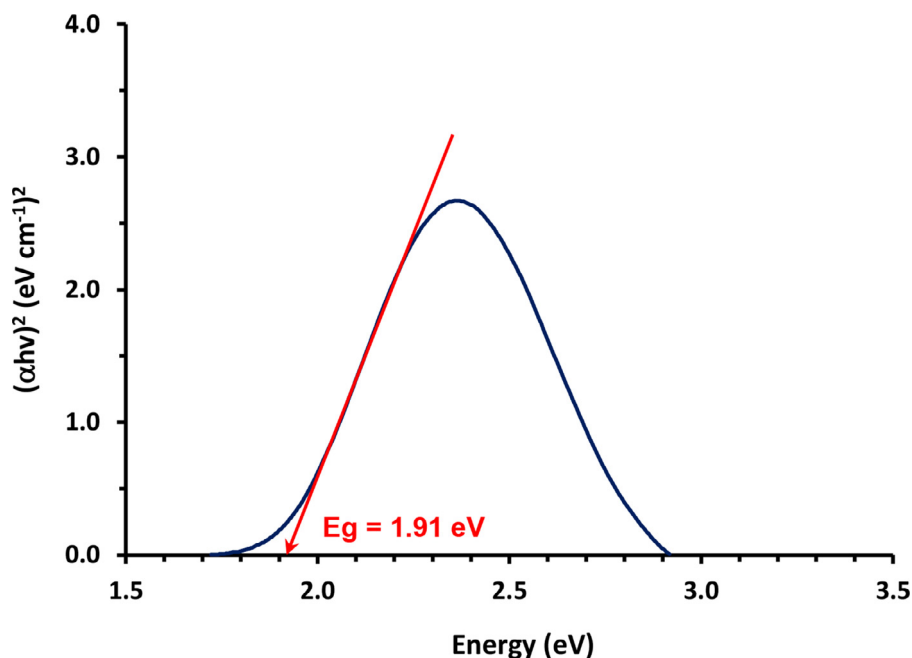


Fig. 2. Tauc plot of energy ($h\nu$) against $(\alpha h\nu)^2$ for the CTC of REM with CLA in methanol.

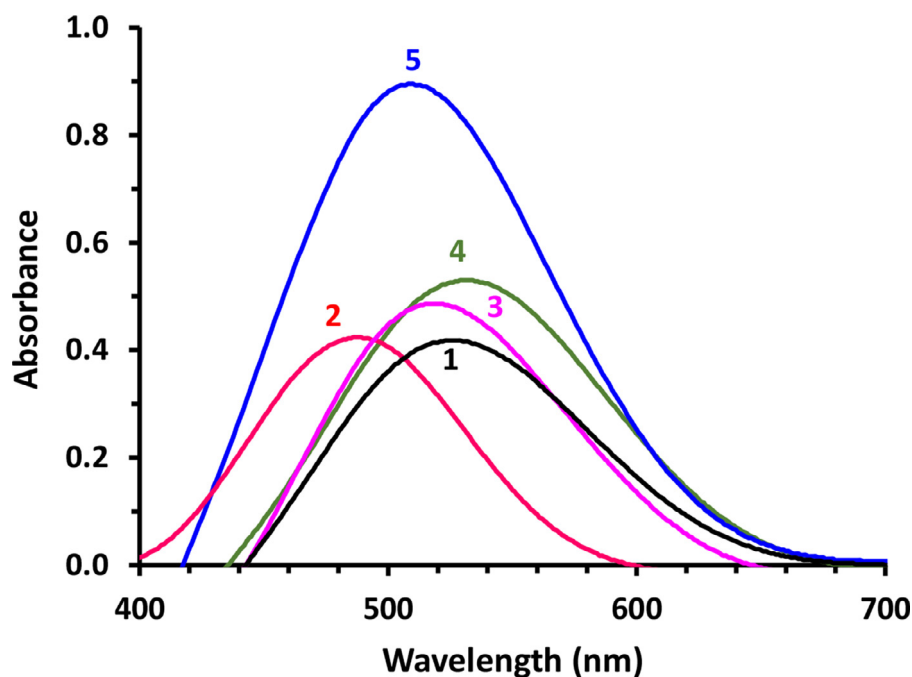


Fig. 3. Effect of solvent on the absorption spectrum of the CTC of REM with CLA. Solvents were diethyl ether (1), dichloroethane (2), chloroform (3), methanol (4) and acetonitrile (5).

$\Delta G^0 = -2.303 RT \log K_c$ where ΔG^0 is the standard free energy change of the complex (Kilo joules; KJ mol^{-1}), R is the gas constant ($8.314 \text{ KJ mole}^{-1}$), T is the absolute temperature in Kelvin ($^\circ\text{C} + 273$) and K_c is the complex association constant (L mol^{-1}). ΔG^0 value was $5.16 \times 10^4 \text{ J mol}^{-1}$. This ΔG^0 value indicates that the interaction between REM and CLA was straightforward, and the CTC was fairly stable [43].

The donor's (REM) ionization potential (I_D) in the CTC of REM with CLA was estimated using Aloisi and Piganatro's empirical equation [44]:

$$I_D(\text{eV}) = 5.76 + 1.53 \times 10^{-4} \nu_{\text{CTC}}$$

where ν_{CTC} is the wave number in cm^{-1} of the CTC, and the ionization potential (I_D) was found to be 9.21 eV.

3.4. Molar ratio and computational charge calculation

Job's continuous variation method [37] was used to determine the molar ratio of REM to CLA, and it was discovered that the REM:CLA ratio was 1:1 (Fig. 6), implying that just one electron-donating site of REM contributed to the formation of the CTC with CLA. To allocate this site among the multiple electron-donating sites available on the REM molecule (Fig. 7), the REM molecule's energy was minimized, and the electron density on each atom was calculated

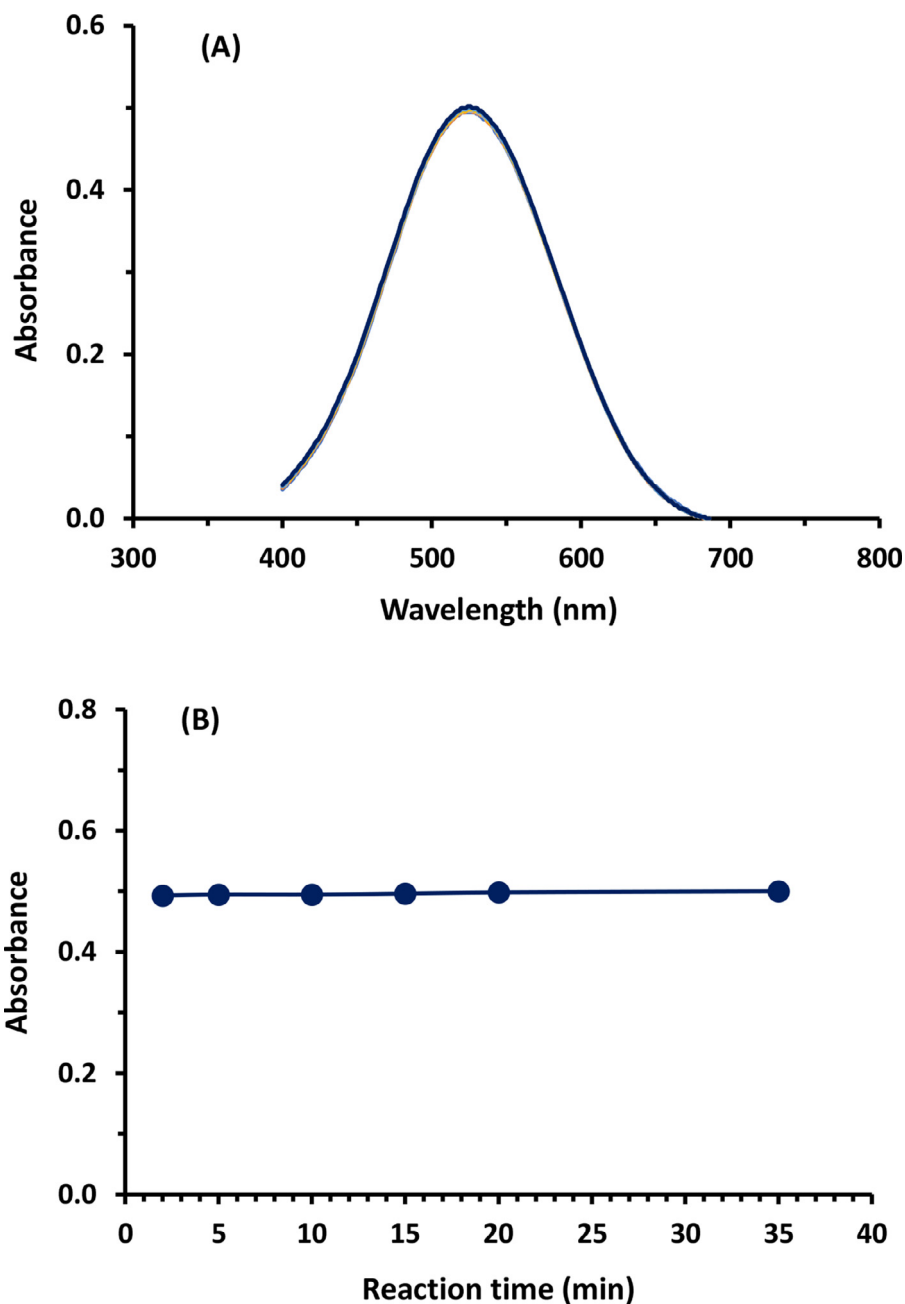


Fig. 4. Panel (A): absorption spectra of reaction mixture containing REM (8×10^{-4} M) and CLA (4×10^{-3} M) at varying reaction times (2–35 min). The spectra are superimposed on each other. Panel (B): the absorbances of the reaction mixture measured at 530 nm plotted against the corresponding reaction time.

directly. The energy minimization and charge calculation were accomplished utilizing CS Chem3D Ultra, version 16.0 (CambridgeSoft Corporation, Cambridge, MA, USA) fulfilled with molecular orbital computations software (MOPAC), and molecular dynamics computations software (MM2 and MMFF94). The results are represented in Table 1. The maximum electron density was found on nitrogen atom taken the number N10 (nitrogen of primary amine attached to pyrolo triazine ring) and nitrogen atom taken the number N25 (nitrogen of secondary amine attached to phosphorous atom). These electron densities were -0.9 and -0.8979 , respectively; the negative signs indicate negative electron densities. These observations, taking the molar ratio in account, suggested that only one nitrogen atom of these two atoms was involved in the formation of the CTC of REM with CLA. To ascertain which nitrogen atom was possibly involved in the reaction, conformational molec-

ular modeling for the CTC was conducted. As shown in Fig. 8, CLA molecule was found near the primary amino group ($-NH_2$) attached to the pyrolo triazine ring indicating that this nitrogen atom was the electron-donating center involved in the formation of CTC between REM and CLA. It is important to note that this computational simulation for the CTC totally neglected the effect of solvent, although it plays a major role in the CT reaction. Thus, this simulation is qualitative in nature, to determine the possible site(s) of interaction and conformation of the complex, which are not affected by the solvent.

The solid-state complex was synthesized and subjected to further spectroscopic and thermal investigations for more confirmation for the site on interaction, and better characterization for the complex.

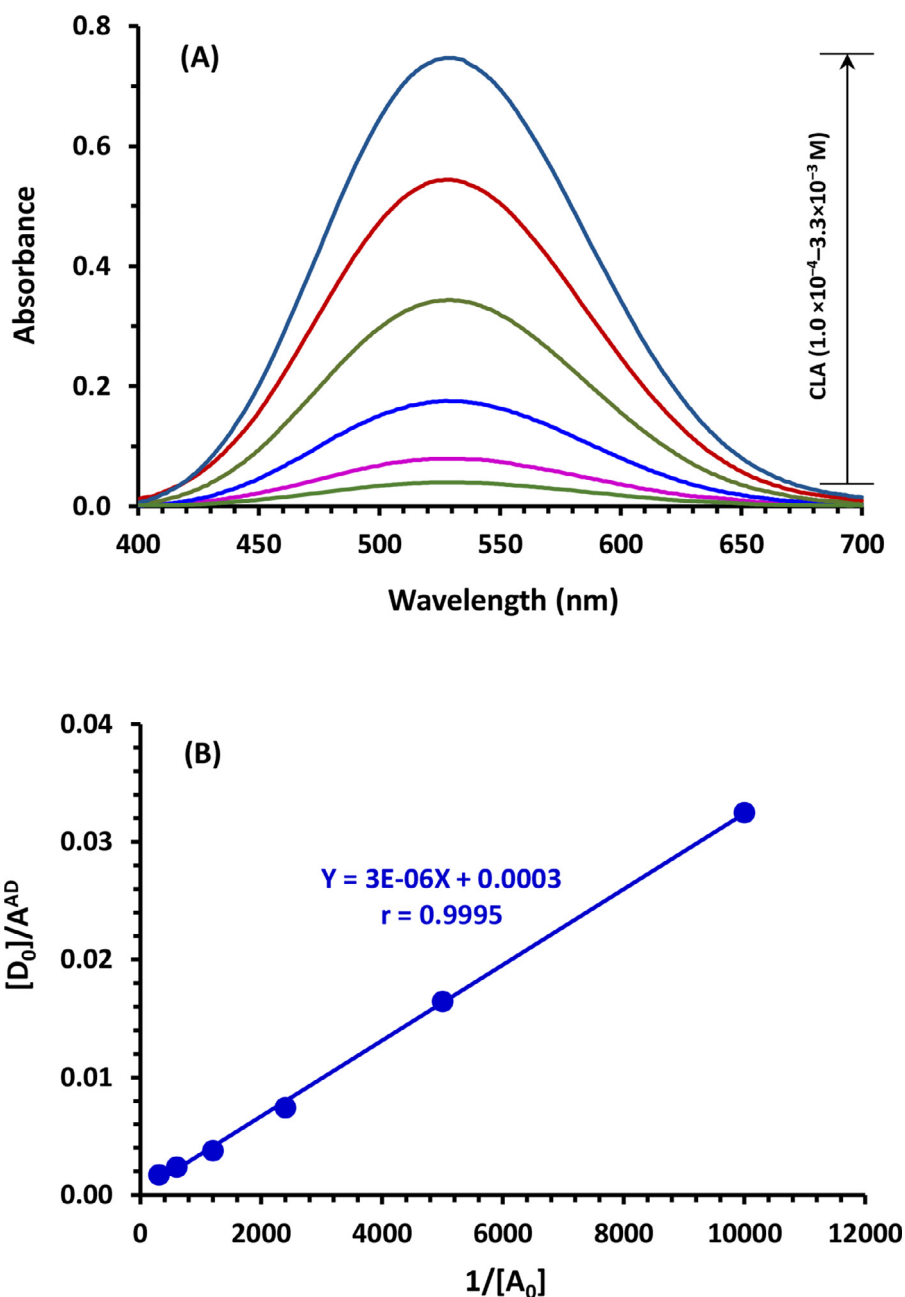


Fig. 5. Panel (A): Absorption spectra of reaction mixtures containing a fixed concentration of REM (1.3×10^{-3} M) and varying concentrations of CLA (1.0×10^{-4} M – 3.3×10^{-3} M) against reagent blank. Panel (B): Benesi-Hildebrand plot for formation of the CTC of REM with CLA. Linear fitting equation and correlation coefficient (r) are given on the plot. $[A_0]$, A^{AD} and $[D_0]$ are the molar concentrations of CLA, absorbances of the complex reaction mixture, and molar concentration of REM, respectively.

3.5. Spectral analysis

3.5.1. FT-IR spectra

FT-IR spectra for CLA, REM, and their CTC were obtained using KBr pellets in the $4000\text{--}400\text{ cm}^{-1}$ range (Fig. 9). The presence of the major characteristic bands of both the donor (REM) and acceptor (CLA) in the CTC's FT-IR spectrum strongly supports the CTC formation. The interpretation of the CTC's FT-IR spectrum was based on changes in intensities and shifts in vibrational frequencies of the formed complex when compared to those of the reactants, REM and CLA [2]. Generally, donor (REM) bands are shifted to lower frequencies while acceptor (CLA) bands are shifted to higher frequencies. These changes in band intensity and shifts or appearance of new bands are due to changes in charge distribution in both REM and CLA molecules upon complexation. The O–H

peak of CLA (appeared at 3229 cm^{-1} in its spectrum) and those of REM (appeared at $3416\text{--}3222\text{ cm}^{-1}$ in the spectrum of REM) were merged together and appeared as broad-band in the spectrum of the complex at 3119 cm^{-1} . This observation eliminated the involvement of O–H of CLA in hydrogen bonding with REM. This assumption was also supported by the existence of O–H protons of CLA in ^1H NMR spectrum of the complex. The peak of $-\text{NH}_2$ group attached to pyrolo triazine ring of REM (appeared at 2960 cm^{-1} in its spectrum) was shifted to a lower frequency in the spectrum of the complex (appeared at 2958 cm^{-1} and overlapped with the sp^3 C–H stretch) without deformation. This observation revealed the involvement of this group in the formation of the complex and further supported that no hydrogen bonding with O–H protons of CLA occurred.

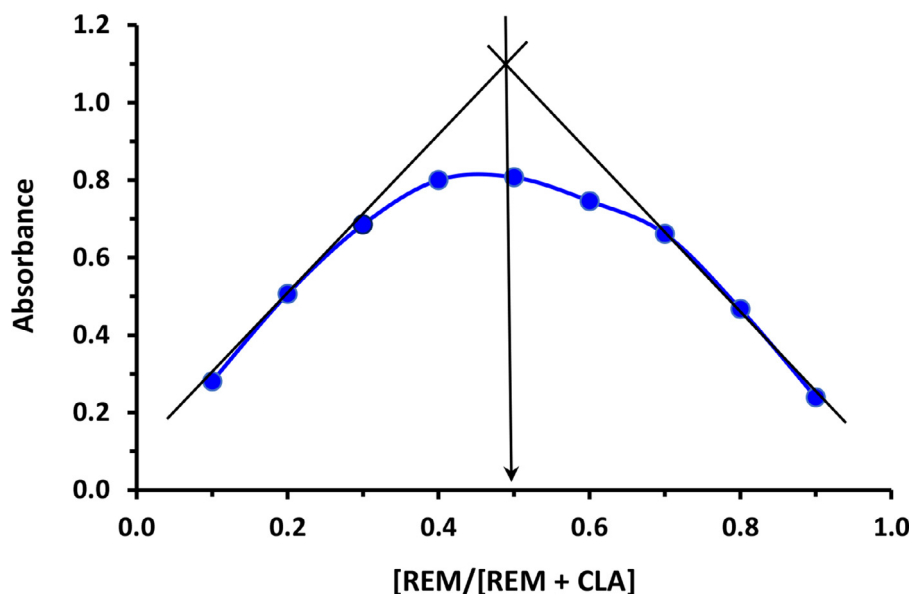


Fig. 6. Job's continuous variation plot for determination of molar ratio of the CT reaction of REM with CLA.

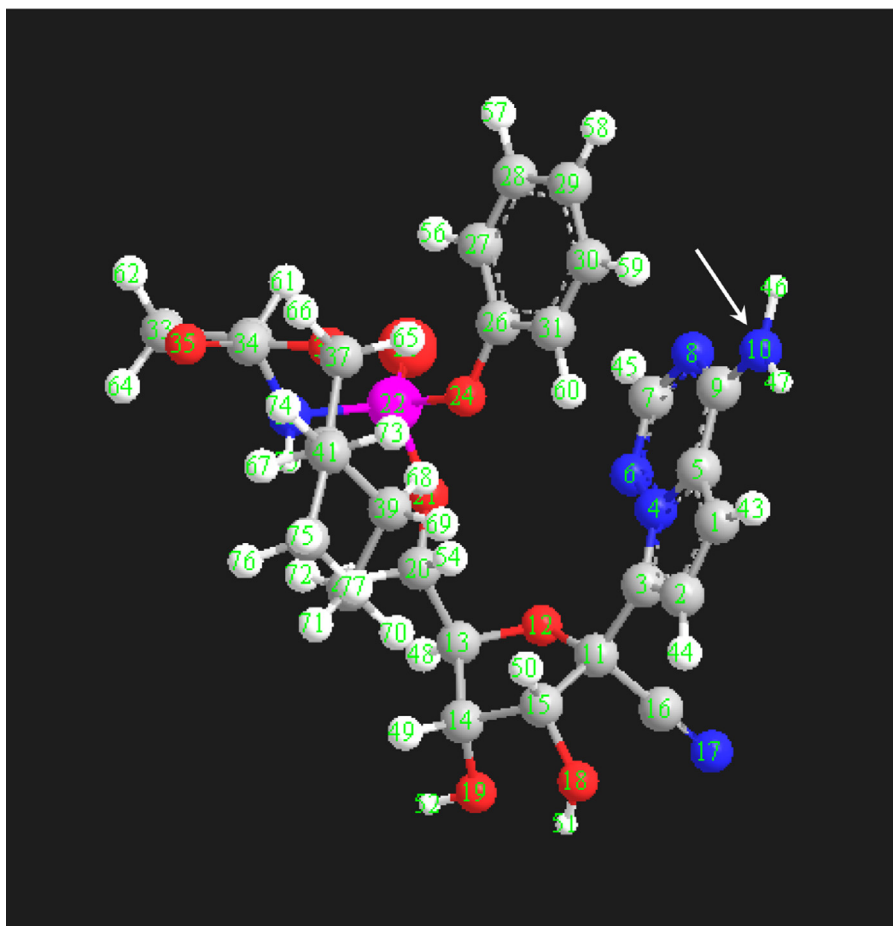


Fig. 7. Energy-minimized REM molecule with atom numbers, arrows point to the atom having the highest electron density (N10).

3.5.2. ^1H NMR spectra

The contribution of $-\text{NH}_2$ group attached to pyrrolo triazine ring to the formation of the complex between REM and CLA was further investigated by analysing their ^1H NMR spectra and that of the complex. The ^1H NMR spectra of REM and CLA obtained in our ex-

periments were typically as found and assigned in previous reports [45,46]. In the spectrum of REM, the protons of $-\text{NH}_2$ group attached to pyrrolo triazine ring appeared at $\sigma = 5.38$ ppm, whereas the peak appeared at $\sigma = 6.05$ ppm in the spectrum of the complex (Fig. 10). In addition, these protons appeared at position very

Table 1
Atom numbers, types, and their calculated charges on the energy-minimized REM molecule.

Atom number	Atom type	Charge	Atom number	Atom type	Charge
C(1)	Aromatic 5-ring C	-0.15	O(23)	O, in phosphine oxide	-0.7
C(2)	Aromatic 5-ring C	-0.15	O(24)	Divalent O, attached to P	-0.3537
C(3)	Aromatic 5-ring C	-0.3316	N(25)	Amine N	-0.8979
N(4)	Aromatic 5-ring N with p lone pair	0.3032	C(26)	Aromatic C, in pyridine	0.0825
C(5)	Aromatic 5-ring C	-0.1516	C(27)-C(31)	Aromatic C, in pyridine	-0.15
N(6)	Imine N	0	C(32)	Alkyl carbon, SP3	0.331
C(7)	Aromatic C, in pyridine	0.16	C(33)	Alkyl carbon, SP3	0
N(8)	Aromatic N, with s lone pair	-0.62	C(34)	Carbonyl C	0.659
C(9)	Aromatic C, in pyridine	0.41	O(35)	Carbonyl O	-0.57
N(10)	Enamine N, delocalized lone pair	-0.9	O(36)	Ether O	-0.43
C(11)	Alkyl C, SP3	0.66	C(37)	Alkyl carbon, SP3	0.28
O(12)	Alcohol or ether O	-0.56	C(38)-C(42)	Alkyl carbon, SP3	0
C(13)-C(15)	Alkyl C, SP3	0.28	H(43)-H(45)	H attached to C	0.15
C(16)	Cyano C	0.3571	H(46)-H(47)	H in H-N-C = N	0.4
N(17)	Triple bonded N	-0.5571	H(48)-H(50)	H attached to C	0
O(18)	Alcohol or ether O	-0.68	H(51)-H(52)	Hydroxyl H in alcohol	0.4
O(19)	Alcohol or ether O	-0.68	H(53)-H(54)	H attached to C	0
C(20)	Alkyl C, SP3	0.28	H(55)	H on SP3 N, in amine	0.36
O(21)	Divalent O, attached to P	-0.5512	H(56)-H(60)	H attached to C	0.15
P(22)	P, with 3 attached O	1.5103	H(61)-H(77)	H attached to C	0

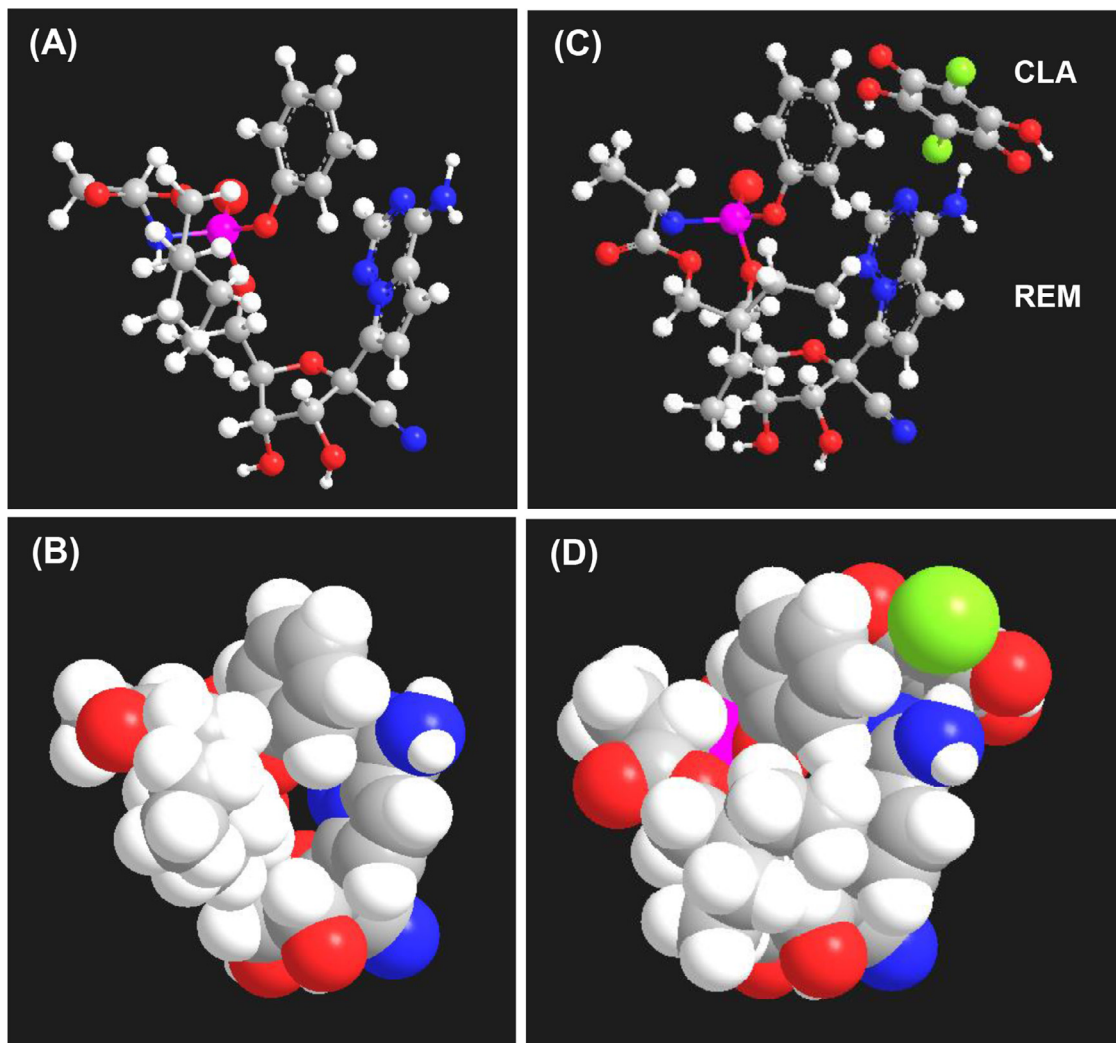


Fig. 8. Energy-minimized conformational and 3D structures REM and its CTC with CLA. Panels A and C are the conformational structures of REM and CTC, respectively. Panels B and D are the 3D structures of REM and CTC, respectively.

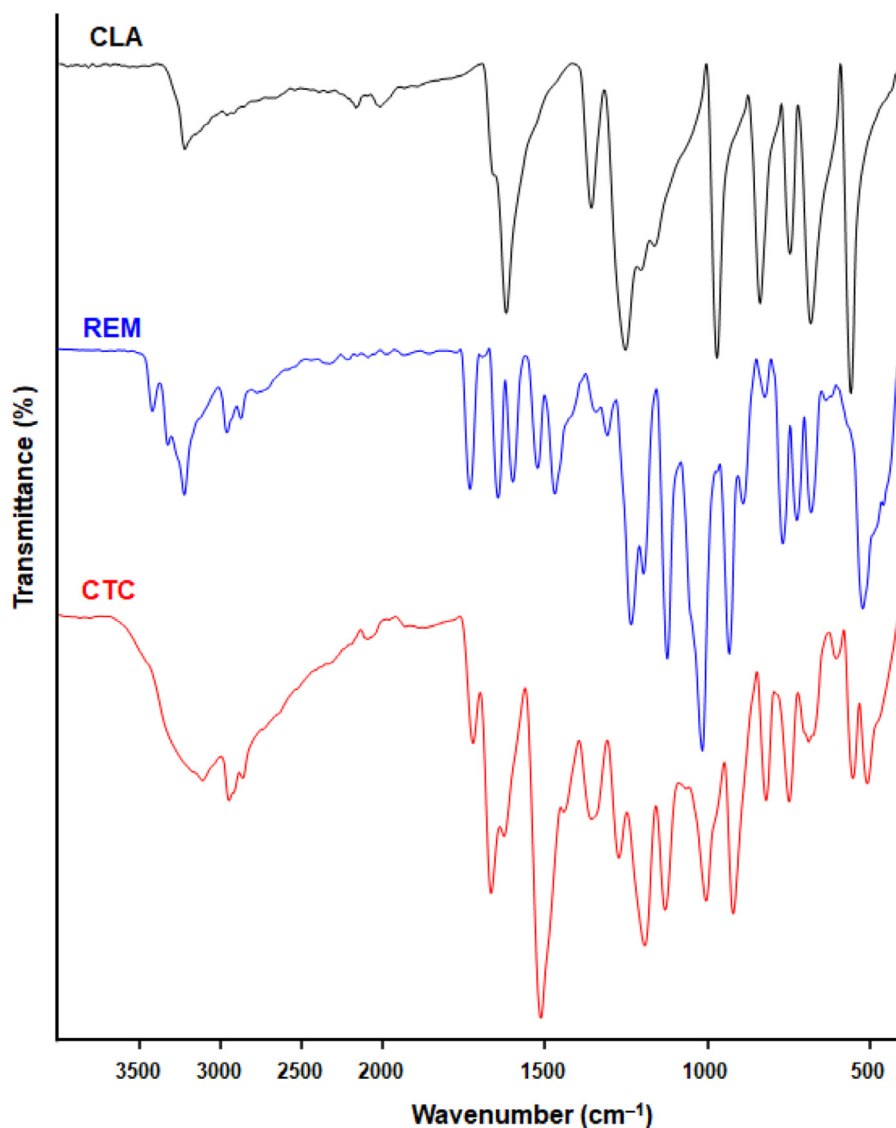


Fig. 9. FT-IR spectra of CLA, REM and their CTC.

close to that of other protons of the pyrolo triazine ring appeared at $\sigma = 6.93 - 7.36$ ppm (Fig. 10).

The mechanism and structure of the CTC of REM and CLA were proposed based on these complementary spectrum data (taking into account the molar ratio of the reaction (1:1)), as shown in Fig. 11.

3.6. Thermogravimetric analysis

For study the thermal property of the CTC of REM with CLA, comparative study of their thermograms were carried (Fig. 12). The Thermogravimetric analysis (TGA) was employed utilizing TGA-8000 thermal analysis in nitrogen atmosphere with a flow rate of 30 mL min^{-1} and heating rate $10 \text{ }^\circ\text{C min}^{-1}$ in the temperature range $50 - 414 \text{ }^\circ\text{C}$, after initial holding for 1 min at $50 \text{ }^\circ\text{C}$, using 0.799, 1.202 and 1.796 mg for REM, CLA and CTC, respectively. The thermogram of CLA and its decomposition behavior was identical to that in the previous report [35]. The thermograms of REM, CLA and the complex exhibited decomposition in one step at 190.04, 196.97 and 186.61 $^\circ\text{C}$, respectively. The weight of CLA was almost complete; however, it was about 55% for REM and the complex.

3.7. Development of MW-SPA

3.7.1. Strategy and design of the assay

Because of its therapeutic value in the treatment of Covid-19, we chose REM as the current study's target medication. The quality of REM's formulation (Valkury® injection) in terms of active component content is critical for its therapeutic benefits. The reported methods for quantitation of REM have been reviewed Y. Pashaei [47]. These methods are mostly liquid chromatography coupled with tandem mass spectrometry (LC-MS/MS) and were described for assessing REM in biological samples, and none of them was not validated for determination of REM in its bulk and/or capsules. Besides, these methods relied on intensive and expensive instruments and complex procedures that do not meet the requirements for analytical methods for quality control of pharmaceuticals. Only one fluorimetric method was described for determination of REM in pharmaceutical dosage form via measuring its native fluorescence [48]. Photometric methodologies are crucial in pharmaceutical analysis because they can easily be automated with photometric analyzers, which are commonly used for serial analysis of pharmaceutical preparations [49]. Obviously, REM chemical structure holds chromophoric moieties (Fig. 10); consequently, it

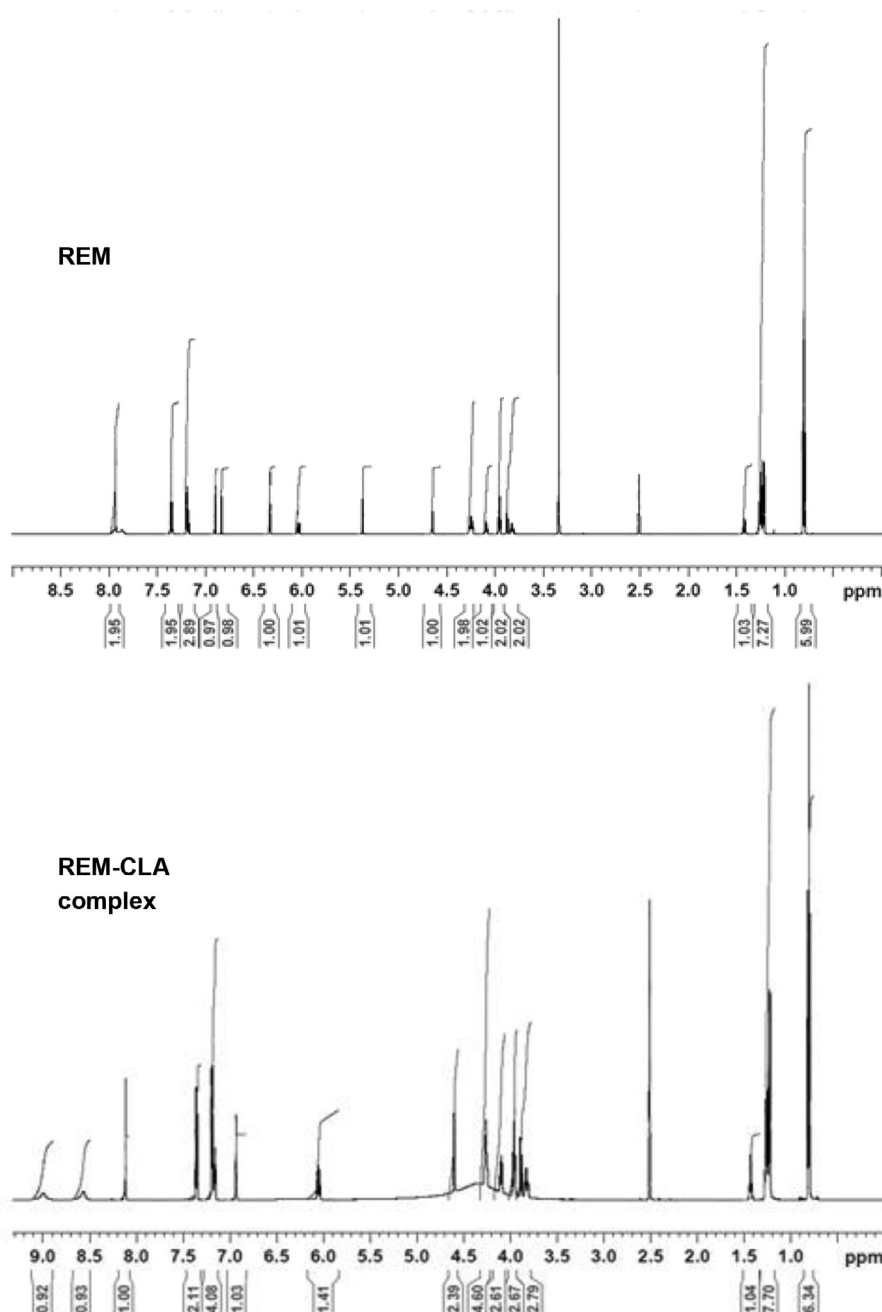


Fig. 10. ^1H NMR spectrum of REM and its CTC with CLA (REM-CLA complex), in DMSO-d_6 .

is expected to display high molar absorptivity. Therefore, developing a photometric method for its quantitation relied on its native ultraviolet (UV) light absorption was possible [50]. However, the availability of a visible photometric method for REM quantitation is imperative to allow its automation with colorimetric analyzer. Based on an extensive review of the available literature, there is no visible photometric method for determination of REM content in its bulk and/or pharmaceutical formulations (injections). Therefore, the current study is dedicated towards the establishment of a visible photometric method to for quantifying REM in its injections. The above-mentioned CT reaction of REM with CLA was behind its usage as a basis in establishing photometric method for REM.

The visible photometric assays based on colored CTC formation and employing the traditional manual technique have limited

throughput [51,52], and furthermore consume large volumes of organic solvents. As a result, these assays are costly, and they also expose the analyst to the harmful impacts of organic solvents [53,54]. Darwish et al. [21–30] previously developed a number of successful microwell-based photometric methods to quantify the active drug contents in pharmaceutical dosage forms using an absorbance plate reader. These methods have a high throughput and use small amounts of organic solvents. As a direct consequence, current efforts are centered on constructing a similar methodology for REM.

3.7.2. Optimization of MW-SPA conditions

Experimental conditions for the success of the reaction in the 96-microwell assay plate were adjusted by modifying each variable in a round while holding the others constant. The reaction was conducted in methanol and all the measurements were employed by the plate reader at 490 nm (the closest filter to the λ_{max} of the

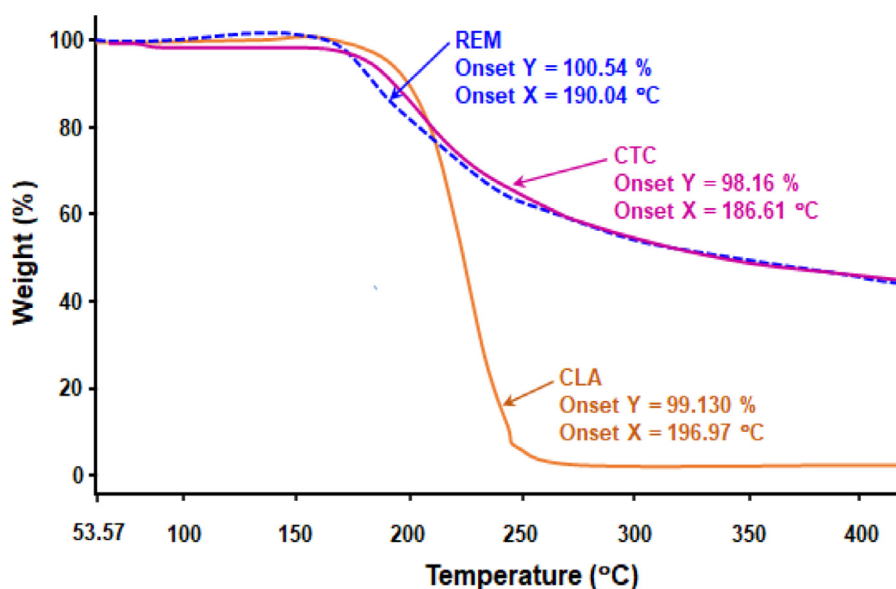


Fig. 12. Thermogravimetric curves of REM, CLA and their CTC.

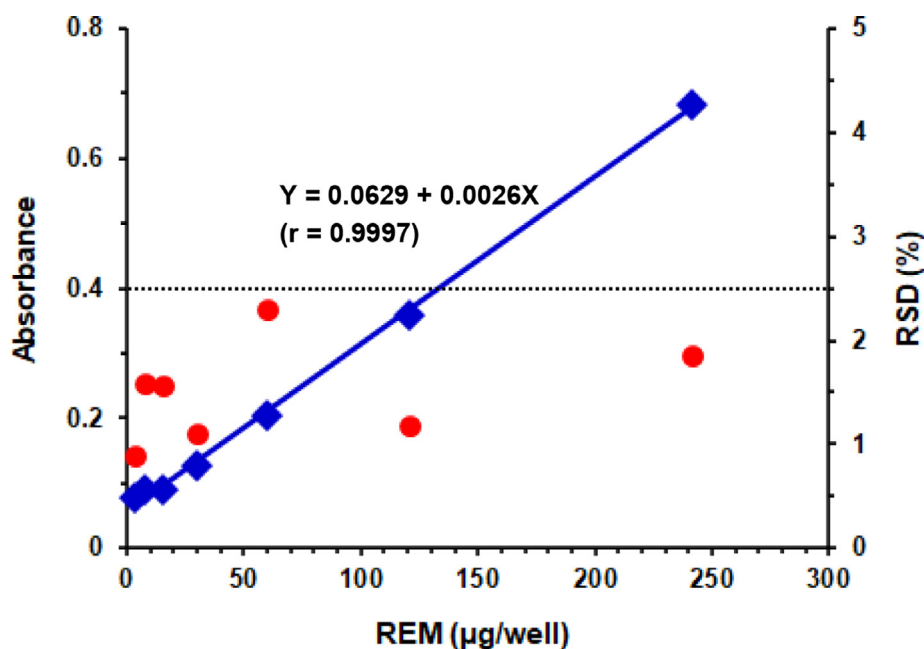


Fig. 13. Calibration curve (♦) and its precision profile (•) for determination of REM by the proposed MW-SPA via formation of CTC with CLA. Linear regression equation and its correlation coefficient (r) is given on the calibration line.

3.8.2. Precision and accuracy

Using samples of REM solution at varying concentration levels, the precisions of the recommended MW-SPA were assessed, and the results are summarized in Table 3. For intra- and inter-assay precision, the relative standard deviations (RSD) were 0.06 – 1.01% and 0.31 – 2.51%, respectively. The assay's good precision was confirmed by these low RSD values. Recovery studies at the same REM concentration levels utilized in the precision studies were conducted to assess the assay accuracy. The recovery values ranged from 98.82 to 102.14 percent (Table 3), demonstrating that the proposed assay is highly accurate.

3.8.3. Specificity and interference

Measurements in the proposed MW-SPA are carried out in the visible range avoiding any potential interference from the UV-absorbing inactive ingredients, which may be extracted from the

pharmaceutical formulation of REM (vaktury® injection). In addition, the assay described in this study involved the extraction of REM from vaktury® injection by methanol; therefore, the excipients/inactive ingredients did not dissolve revealing the specificity of the assay.

3.9. Application of MW-SPA to the quantitation of REM in vaktury® injection

The impactful validation results made the proposed MW-SPA beneficial use to determine REM in vaktury® injection. The mean value of the labelled amount obtained was $99.74 \pm 1.02\%$. This result demonstrated that the proposed MW-SPA is suitable for quantifying REM in injection.

Table 3
Precision and accuracy of the proposed MW-SPA at different REM concentration levels.

Taken concentration ($\mu\text{g/well}$)	Precision: relative standard deviation (%)		Accuracy: recovery (% \pm SD)
	Intra-assay, $n = 5$	Inter-assay, $n = 6$	
12.5	0.90	2.51	101.12 \pm 1.02
25	0.67	2.18	99.58 \pm 0.87
50	0.31	2.15	100.48 \pm 1.23
100	0.06	0.31	98.82 \pm 2.05
200	1.01	0.81	102.14 \pm 1.57

^a Values are mean of three determinations.

4. Conclusions

UV-visible study demonstrated the formation of CTC of REM and CLA, as revealed by the appearance of a new unique absorption band at 530 nm in their reaction in methanol. The complex's molecular stoichiometry was determined to be 1:1. The λ_{max} and ϵ of the complex were dependent on both the polarity index and the dielectric constant of the solvent utilized for the reaction. The site of interaction on REM molecules that contributed to the formation of the complex was suggested via computational charge calculation and molecular modeling. Both FT-IR and ^1H NMR spectroscopy confirmed the formation of the complex via CT reaction, and also confirmed the reaction mechanism. In this study, the interaction between REM and CLA was developed to serve as the basis for a novel 96-microwell spectrophotometric assay for the quantification of REM in both bulk and injection. The assay described in this study is considered the first microwell-based spectrophotometric assay for REM. The assay is characterized by high throughput which allows for the analysis of large sample size in a short period of time. It also has the advantage of being environmentally friendly when used in pharmaceutical quality control laboratories because it only requires a little amount of organic solvent to be proceeded.

Declaration of Competing Interest

The authors state that they have no recognized competing financial interests or personal connections that could have influenced the research presented in this study.

CRediT authorship contribution statement

Ibrahim A. Darwish: Conceptualization, Methodology, Resources, Supervision, Writing – review & editing. **Nasr Y. Khalil:** Investigation, Visualization, Data curation, Validation, Formal analysis. **Hany W. Darwish:** Investigation, Visualization, Data curation, Writing – review & editing. **Nourah Z. Alzoman:** Data curation, Writing – review & editing. **Abdullah M. Al-Hossaini:** Investigation, Data curation, Writing – review & editing.

Acknowledgments

The authors would like to extend their appreciation to the Deanship of Scientific Research at King Saud University for its funding of this research through the research group project No. RGP-225.

References

- [1] R.S. Mulliken, W.B. Pearson, *Molecular Complexes*, Wiley Publishers, New York, 1969.
- [2] R. Foster, *Organic Charge-Transfer Complexes*, Academic Press, London, 1969.
- [3] S.K. Das, G. Krishnamorthy, S.K. Dofra, *Can. J. Chem.* 78 (2000) 191–205.
- [4] A.S. Datta, S. Bagchi, A. Chakraborty, S.C. Lahiri, *Spectrochim. Acta A* 146 (2015) 119–128.
- [5] H. Liu, Z. Liu, W. Jiang, H. Fu, *J. Solid State Chem.* 274 (2019) 47–51.
- [6] V. Murugesan, M. Saravanabhavan, M. Sekar, *J. Photochem. Photobiol. B* 140 (2014) 20–27.
- [7] N. Singh, I.M. Khan, A. Ahmad, S. Javed, *J. Mol. Struct.* 1056–1066 (2014) 74–85.
- [8] A.S.A. Almalki, A. Alhadhrami, A.M.A. Adam, I. Grabchev, M. Almeataq, J.Y. Al-Humaidi, T. Sharshar, M.S. Refat, *J. Photochem. Photobiol. A* 361 (2018) 76–85.
- [9] A.S.A. Almalki, A. Alhadhrami, R.J. Obaid, M.A. Alsharif, A.A. Adam, I. Grabchev, M.S. Refat, *J. Mol. Liq.* 261 (2018) 565–582.
- [10] F. Yakuphanoglu, M. Arslan, *Solid State Commun.* 132 (2004) 229–234.
- [11] F. Yakuphanoglu, M. Arslan, *Opt. Mater.* 27 (2004) 29–37.
- [12] F. Yakuphanoglu, M. Arslan, M. Kucukislamoglu, M. Zengin, *Sol. Energy* 79 (2005) 96–100.
- [13] B. Chakraborty, A.S. Mukherjee, B.K. Seal, *Spectrochim. Acta A* 57 (2001) 223–229.
- [14] S.M. Andrade, S.M.B. Costa, R. Pansu, *J. Colloid Interface Sci.* 226 (2000) 260–268.
- [15] R. Dabestani, K.J. Reszka, M.E. Sigman, *J. Photochem. Photobiol. A* 117 (1998) 223–233.
- [16] R. Jakubiak, Z. Bao, L. Rothberg, *Synth. Met.* 114 (2000) 61–64.
- [17] K. Takahashi, K. Horino, T. Komura, K. Murata, *Bull. Chem. Soc. Jpn.* 66 (1993) 733–738.
- [18] A. Eychmuller, A.L. Rogach, *Pure Appl. Chem.* 72 (2000) 179–188.
- [19] I.A. Darwish, T.A. Wani, N.Y. Khalil, A.A. Al-Majed, *Int. J. Res. Pharm. Sci.* 1 (2010) 391–395.
- [20] G.A. Saleh, H.F. Askal, I.A. Darwish, A.A. El-Shorbagi, *Anal. Sci.* 19 (2003) 281–287.
- [21] I.A. Darwish, J.M. Alshehri, N.Z. Alzoman, N.Y. Khalil, H.M. Abdel-Rahman, *Lat. Am. J. Pharm.* 33 (2014) 928–934.
- [22] I.A. Darwish, J.M. Alshehri, N.Z. Alzoman, N.Y. Khalil, H.M. Abdel-Rahman, *J. Soln. Chem.* 43 (2014) 1282–1295.
- [23] I.A. Darwish, T.A. Wani, N.Y. Khalil, H.M. Abdel-Rahman, *Acta Pharm.* 64 (2014) 63–75.
- [24] I.A. Darwish, T.A. Wani, M.A. Alqarni, S.R. Ahamed, *Lat. Am. J. Pharm.* 33 (2014) 587–594.
- [25] N.Y. Khalil, T.A. Wani, I.A. Darwish, I.S. Assiri, *Trop. J. Pharm. Res.* 14 (2015) 1667–1672.
- [26] N.Z. Alzoman, M.A. Sultan, H.M. Maher, M.M. Alshehri, T.A. Wani, I.A. Darwish, *Molecules* 18 (2013) 7711–7725.
- [27] I.A. Darwish, T.A. Wani, N.Y. Khalil, A. Al-Shaikh, N. Al-Morshadi, *Chem. Cent. J.* 6 (2012) 1–7.
- [28] T.A. Wani, A. Ahmad, S. Zargar, N.Y. Khalil, I.A. Darwish, *Chem. Cent. J.* 6 (2012) 1–9.
- [29] I.A. Darwish, H.W. Darwish, N.Y. Khalil, A.Y.A. Sayed, *Molecules* 26 (2021) 744.
- [30] I.A. Darwish, N.Y. Khalil, H.W. Darwish, N.Z. Alzoman, A.M. Al-Hossaini, *Spectrochimica Acta Part A* 252 (2021) 119482.
- [31] U.S. Food & Drug Administration. FDA Approves First Treatment for Ebola Virus. <https://www.fda.gov/news-events/press-announcements/fda-approves-first-treatment-ebola-virus>. Assessed: March 4, 2022.
- [32] European Medicines Agency, Veklury: remdesivir. (2022) <https://www.ema.europa.eu/en/medicines/human/EPAR/veklury>. Assessed: Jan. 10.
- [33] U.S. Food & Drug Administration. FDA Approves First Treatment for COVID-19. <https://www.fda.gov/news-events/press-announcements/fda-approves-first-treatment-covid-19>. Assessed: March 4, 2022.
- [34] I.A. Darwish, *Anal. Chim. Acta* 549 (2005) 212–220.
- [35] I.A. Darwish, A.A. Almelhizia, A.Y. Sayed, N.Y. Khalil, N.Z. Alzoman, H.W. Darwish, *Spectrochimica Acta A* 264 (2022) 120287.
- [36] H.A. Benesi, J. Hildebrand, *J. Am. Soc.* 71 (1949) 2703–2703.
- [37] P. Job, *Ann. Chem.* 16 (1963) 97.
- [38] G.A. Gohar, M.M. Habeeb, *Spectroscopy* 14 (2000) 99–107.
- [39] F. Karipcin, B. Dede, Y. Caglar, D. Hür, S. Ilcan, M. Caglar, Y. Şahin, *Opt. Commun.* 272 (2007) 131–137.
- [40] P. Makula, M. Pacia, W. Macyk, *J. Phys. Chem. Lett.* 9 (2018) 6814–6817.
- [41] A.I. Vogel, A.R. Tatchell, B.S. Furnis, A.J. Hannaford, P.G. Smith, *Vogel's Textbook of Practical Organic Chemistry*, 5th ed., Longman Group UK Ltd., England, 1989.
- [42] Polarity Index. <http://macro.lsu.edu/howto/solvents/polarity%20index.htm>. Assessed: March 4, 2022.
- [43] M. Pandeewaran, K. Elango, *Spectrochim. Acta A* 65 (2006) 1148–1153.
- [44] G. Aloisi, S. Pignataro, *J. Chem. Soc. Faraday Trans.* 69 (1972) 534–539.
- [45] S. Sahakijijarn, C. Moon, J.J. Koleng, D.J. Christensen, R.O. Williams III, *Pharmaceutics* 12 (2020) 1002.

- [46] S.I. Mostafa, *Transition Met. Chem.* 24 (1999) 306–310.
- [47] Y. Pashaei, *Drug Discov. Ther.* 14 (2020) 273–281.
- [48] H. Elmansi, A.E. Ibrahim, I.E. Mikhail, F. Belal, *Anal. Methods* 13 (2021) 2596–2602.
- [49] S. Görög, *Ultraviolet-Visible Spectrophotometry in Pharmaceutical Analysis*, CRC Press, New York, 2018.
- [50] I. Bulduk, E. Akbel, J. Taibah *Univ. Sci.* 15 (2021) 507–513.
- [51] A. Gouda, *Int. J. Pharm. Pharm. Sci.* 6 (2014) 334–341.
- [52] I.A. Darwish, I.A. Refaat, *J. AOAC Int.* 89 (2006) 362–333.
- [53] H. Wennborg, J.P. Bonde, M. Stenbeck, J. Olsen, *Scand. J. Work Environ. Health* 28 (2002) 5–11.
- [54] P. Kristensen, B. Hilt, K. Svendsen, T.K. Grimsrud, *Eur. J. Epidemiol.* 23 (2008) 11–15.
- [55] *The International Conference on Harmonization (ICH)Q2(R1): Validation of Analytical procedure: Text and Methodology*, ICH, Geneva, 2005.